

Example Problem CO2-7

Viscous Fingering with Dissolution of CO₂ into Brine

Abstract: *CO₂ injected into saline reservoirs partitions into a CO₂-dominate phase (gas phase) and CO₂ dissolved in the aqueous brine. The gas phase is generally less dense than the aqueous brine yielding an upward buoyant force on the gas phase, causing it to rise with respect to the aqueous phase. When the gas phase encounters a low permeability obstruction it spreads laterally beneath the obstruction. CO₂ in the gas phase moving laterally beneath the obstruction dissolves into the aqueous brine in contact with the gas phase. When CO₂ dissolves into an aqueous brine phase, the resulting brine is up to 1% denser than the CO₂-free brine. Whereas the lesser dense gas phase is stable over the aqueous brine as it moves laterally beneath an obstruction, the resulting layer of denser CO₂-rich aqueous brine is not stable over the lesser dense CO₂-free aqueous brine {i.e., Rayleigh-Taylor instability, (Rayleigh, 1883; Taylor, 1950)}. This problem involves the development of Rayleigh-Taylor instability for two scenarios involving the dissolution of CO₂ into an aqueous phase. The first scenario involves two-phase (i.e., liquid-CO₂-aqueous) conditions and the second involves aqueous-saturated (i.e., no gas) conditions. The second scenario is one which has been compared with experiments conducted at the Masdar Institute in Abu Dhabi.*

Problem Description

This problem involves two scenarios. The first scenario considers the injection of liquid (liq-CO₂) into a laboratory-scale flow cell filled with quartz sand of uniform grain size. The second scenario considers the formation of viscous fingers from a nonuniform initial distribution of aqueous dissolved CO₂. In the first scenario, viscous finger formation is triggered without introducing initial heterogeneities and in the second scenario the initial heterogeneities trigger early-time finger formation. Exercises for this problem are only associated with the first scenario, as the second scenario requires more time to execute than reasonable for a short-course problem. Simulation results are presented and discussed for the second scenario, but the student is not expected to execute the second scenario simulation during the short course period. The first scenario will be described first, followed by the second.

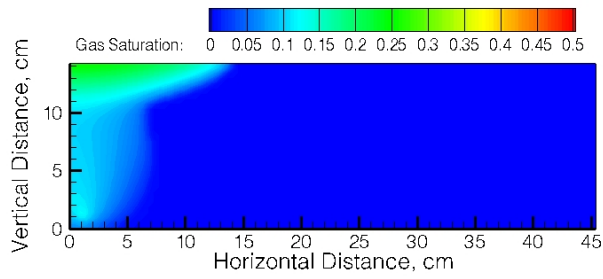
Scenario 1: Pressure Cell

In this scenario, liq-CO₂ is injected into the lower left-hand corner of a rectangular flow cell [45.4 cm (w) × 14.29 cm (h) × 1.27 cm (d)] filled with 30/40 Accusand. CO₂ is injected under supercritical pressure conditions, but below supercritical temperature conditions, causing the CO₂ to be in the liquid-CO₂ state. CO₂ is injected at a rate of 8.5816 cm³/hr for 4 hours. The injected CO₂ is then allowed to redistribute for an additional 2 hours. To maintain constant pressure conditions in the flow cell, a pressure port is implemented in the upper right-hand corner of the flow cell. The hydrologic properties of the 30/40 Accusands are listed in Table 1, where the saturation-capillary pressure function is that of Brooks and Corey (1964, 1966), the aqueous relative permeability function that of Brooks and Corey (1964, 1966) with the Burdine (1953) porosity distribution model, and the gas relative permeability that of Corey (1954).

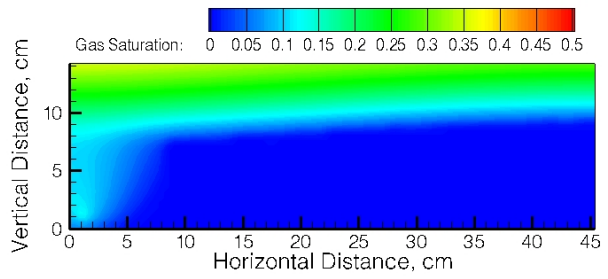
CO₂ injected into the lower left-hand port, located at the lower left-hand node, forms a gas phase, which spreads slightly laterally, but generally vertically via the buoyancy of the gas. The constant pressure port at the upper right-hand node of the domain is specified with a Dirichlet-type boundary condition for the aqueous and gas phases. During the injection period gas continues to migrate vertically until it reaches the upper flow-cell cap; where it migrates laterally beneath the upper cap. After injection stops the gas phase forms a layer underneath the flow-cell cap. Gas saturation profiles at 1 through 6 hours are shown in Figure 1. The capillary fringe between the aqueous and gas phases in the profile at 6 hours is located approximately at the 10-cm height level. Whereas the gas saturation profiles look smooth and predictable throughout the simulation, the profiles of CO₂ dissolved in the aqueous phase, shown in Figure 2, are dominated by fingers of descending CO₂ saturated plumes. The initiation of the fingering is largely impacted by the computational grid as can be seen in the CO₂ aqueous mass fraction profile at 2 hours, in Figure 2b. This implies that for this simulation scenario the resulting fingering profiles are dependent on the grid structure. The strong development of the fingered structures over the short time period of 6 hours is a function of the small domain size of the problem. Such rapid viscous fingering structures would not be expected to form over such short time periods for field-scale geologic sequestration scenarios.

Table 1. Hydrologic Properties of 30/40 Accusands

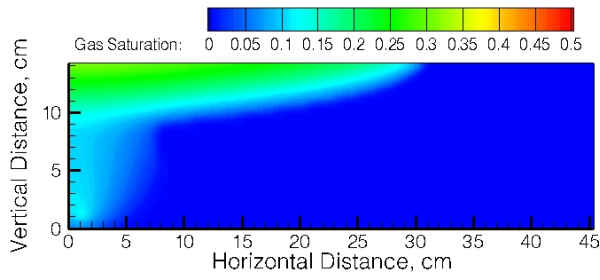
Property	30/40 Accusands
Grain Density	$\rho_g = 2650 \text{ kg} / \text{m}^3$
Porosity	$\phi = 0.327$
Hydraulic Conductivity	$K = 6.95 \text{ cm} / \text{min}$
Intrinsic Permeability	$k = 1.2036 \times 10^{-10} \text{ m}^2$
Sat.- Cap. Press. Func.	$\bar{s}_l = \left(\frac{s_l - s_{lr}}{1 - s_{lr}} \right) = \left(\frac{\psi}{\beta_{gl} h_{gl}} \right)^\lambda$
Gas Entry Pressure Head	$\psi = 19.06815 \text{ cm}$
Exponent Coefficient	$\lambda = 8.476029$
Aqu. Residual Saturation	$s_{lr} = 0.052$
Aqu. Rel. Perm. Function	$k_{rl} = (\bar{s}_l)^{\left(3 + \frac{2}{\lambda}\right)}$
Exponent Coefficient	$\lambda = 8.476029$
Gas Rel. Perm. Function	$k_{rg} = \left[(1 - \bar{s}_l)^2 \right] \left[1 - (\bar{s}_l)^2 \right]$



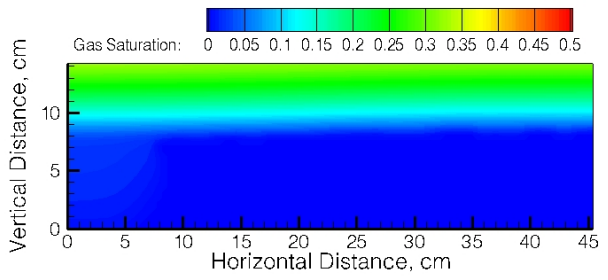
1a



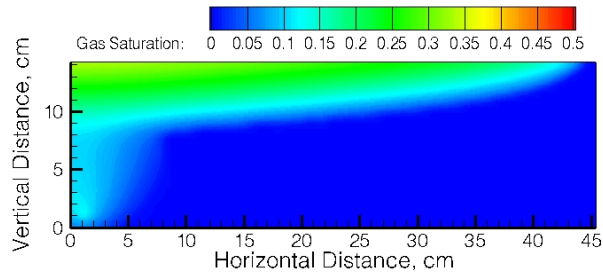
1d



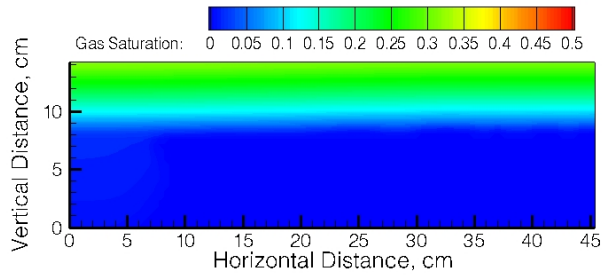
1b



1e



1c



1f

Figure 1. Scenario 1: Gas Saturation Profiles at 1, 2, 3, 4, 5, and 6 Hours in 1a, 1b, 1c, 1d, 1e, and 1f, Respectively

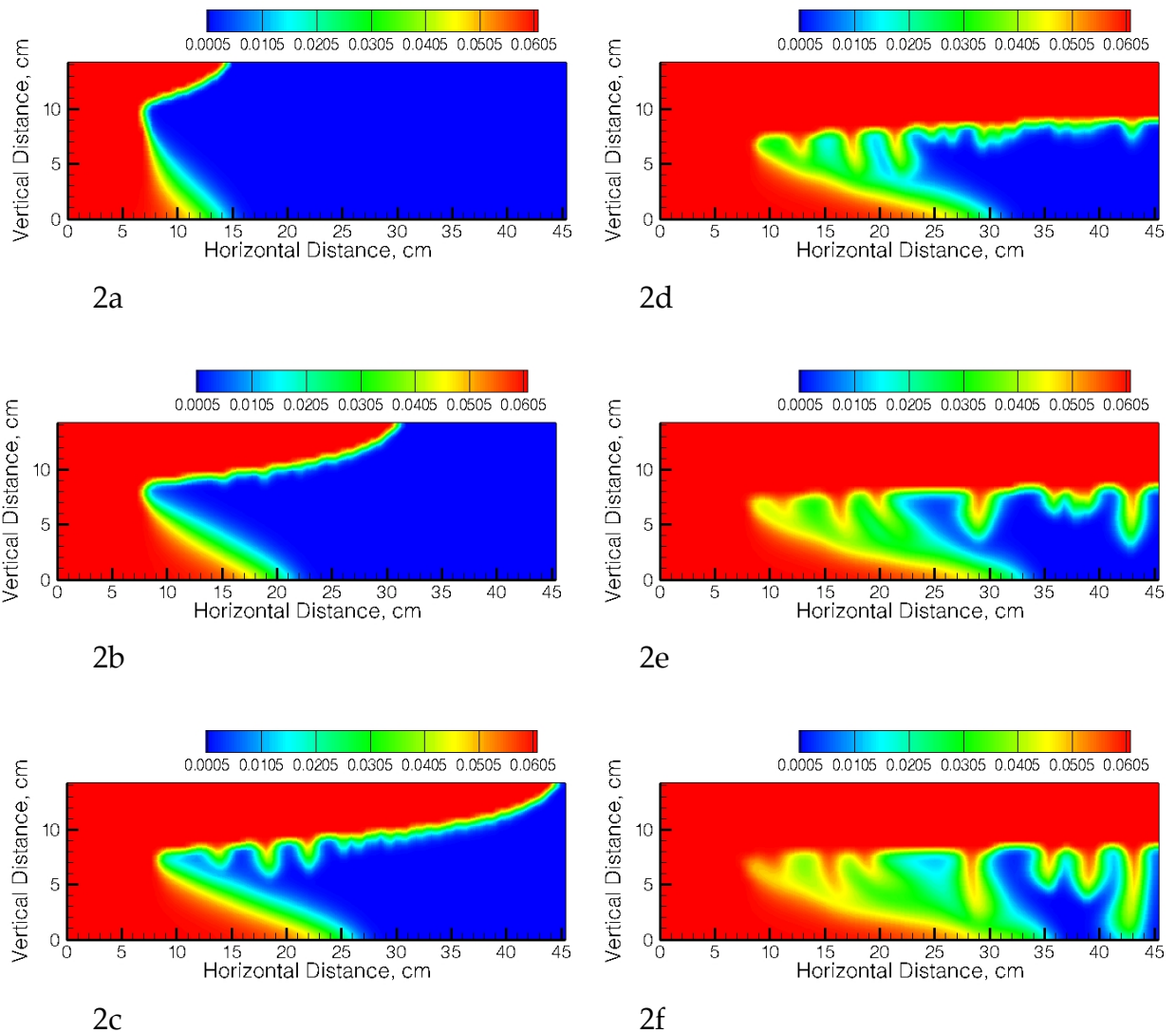


Figure 2. Scenario 1: CO₂ Aqueous Mass Fraction Profiles at 1, 2, 3, 4, 5, and 6 Hours in 2a, 2b, 2c, 2d, 2e, and 2f, Respectively

Scenario 2: Hele-Shaw Cell

In this scenario, a Hele-Shaw cell of 10-m (width) x 20-m (height) is modeled as a 2-dimensional flow cell filled with a porous media. The flow cell is initialized with a stepped distribution of dissolved aqueous CO₂ across the top of the flow cell. The aqueous and gas pressures are set equal to each other, creating aqueous saturated conditions throughout the domain (i.e., no gas phase). The temperature is initialized to 45°C and an initial salt concentration of 100 kg/m³ aqueous is specified. CO₂ is continually added to the top of the domain by the use of an initial condition boundary

condition for the aqueous phase, which includes the dissolved CO₂ concentration. The hydrologic properties of the porous media inside the domain modeling the Hele-Shaw cell are listed in Table 2, where the saturation-capillary pressure function is that of van Genuchten (1980), the aqueous relative permeability function that of van Genuchten (1980) with the Mualem porosity distribution model, and the gas relative permeability function that of van Genuchten (1980) with the Mualem porosity distribution model.

Table 2. Hydrologic Properties of Porous Media Modeling the Hele-Shaw Cell

Property	30/40 Accusands
Grain Density	$\rho_g = 2650 \text{ kg} / \text{m}^3$
Porosity	$\phi = 0.327$
Storativity	$S = 4.5 \times 10^{-6} \text{ 1} / \text{m}$
Intrinsic Permeability	$k_x = 1.0 \times 10^{-11} \text{ m}^2; k_z = 1.0 \times 10^{-11} \text{ m}^2$
Sat.- Cap. Press. Func.	$\bar{s}_l = \left[1 + (\alpha h)^n \right]^{-m}; m = 1 - \frac{1}{n}; \bar{s}_l = \frac{s_l - s_{lr}}{1 - s_{lr}}$
Inverse Entry Head	$\alpha = 0.2 \text{ cm}^{-1}$
Exponent Coefficients	$n = 1.8; m = 0.444$
Aqu. Residual Saturation	$s_{lr} = 0.0$
Aqu. Rel. Perm. Function	$k_{rl} = \sqrt{\bar{s}_l} \left[\left(1 - \left(1 - (\bar{s}_l)^{1/m} \right)^m \right)^2 \right]$
Gas Rel. Perm. Function	$k_{rg} = \sqrt{(1 - \bar{s}_l)} \left[\left(\left(1 - (\bar{s}_l)^{1/m} \right)^m \right)^2 \right]$

The dissolved CO₂ concentration is initialized in a dental pattern at the top of the domain, which generates the initial fingering as shown in Figure 3a, after 50 days. The viscous finger migration then proceeds with the upper boundary providing a constant

source of aqueous dissolved CO_2 in the same dental pattern as used initially. The downward migration is slower than for Scenario 1, as the Hele-Shaw cell is meso-scale size (i.e., 10s of meters) and the pressure cell is laboratory-scale size (i.e., meters). As the simulation progresses the individual fingers coalesce together forming larger fingers with a faster descension rate, with the largest finger contacting the bottom of the Hele-Shaw cell around 800 days.

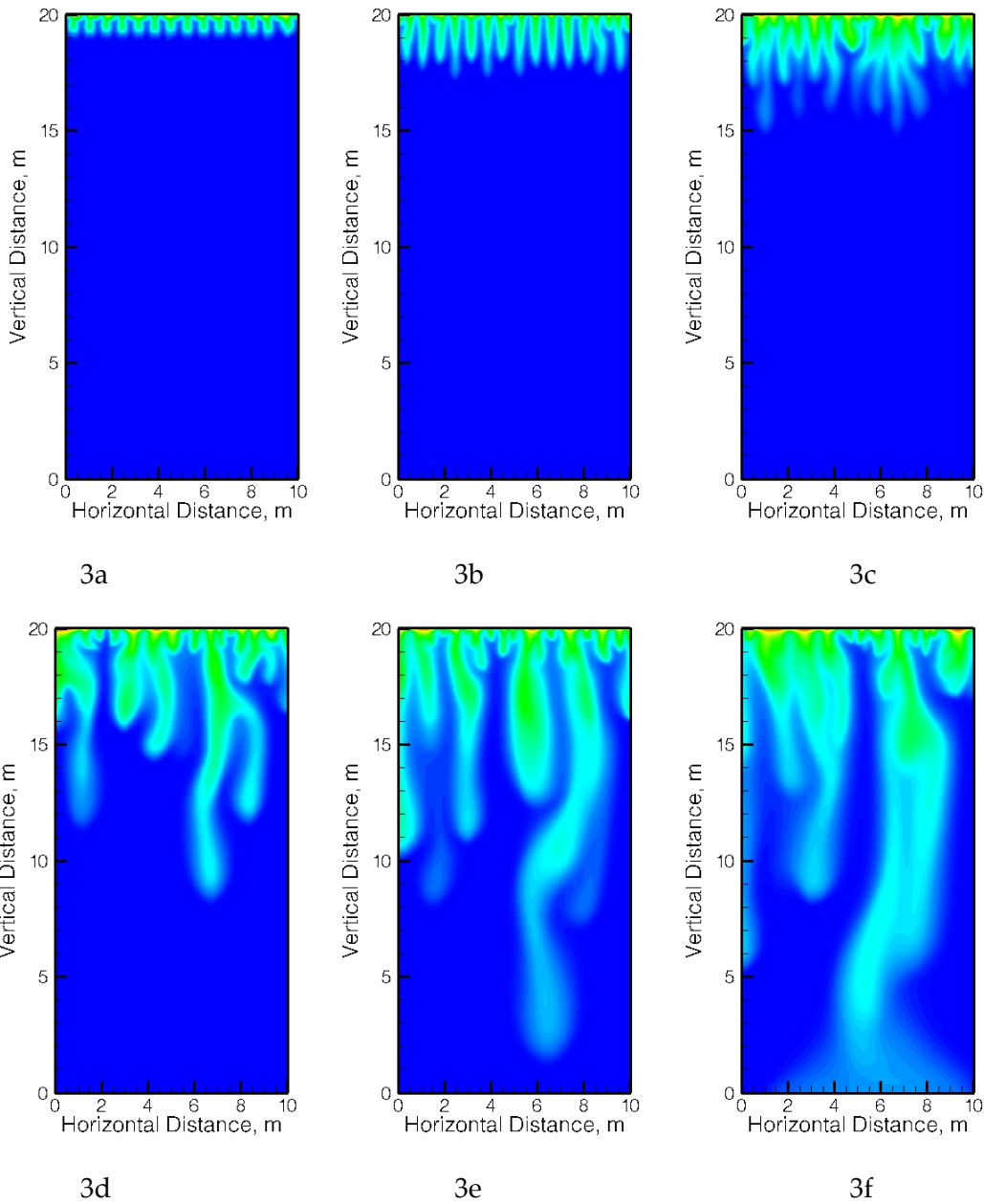


Figure 3. Scenario 2: CO_2 aqueous mass fraction profiles at 50, 100, 200, 400, 600 and 800 days in 3a, 3b, 3c, 3d, 3e, and 3f, respectively.

References

Brooks, R. H., Corey, A. T., 1964. "Hydraulic Properties of Porous Media." *Colorado State University, Hydrology Paper, No. 3*, Fort Collins, Colorado.

Brooks, R. H., and A. T. Corey. 1966. "Properties of porous media affecting fluid flow." *Journal of Irrigation and Drainage Division* 93(3):61-88.

Burdine, N.T. 1953. "Relative permeability calculations from pore-size distribution data." *Petroleum Trans.* 198:71-77.

Corey, A.T. 1954. "The Interrelation Between Gas and Oil Relative Permeabilities". *Prod. Monthly* **19** (1): 38–41.

van Genuchten, M. T. A. 1980. "A closed-form equation for predicting the hydraulic conductivity of unsaturated soils." *Soil Sci. Soc. Am. J.*, 44:892-898.

Exercises

1. (Moderate) Repeat the pressure-cell simulation, but using invariant aqueous density and viscosity. Determine an appropriate aqueous density and viscosity from a zero-time-step simulation, using the original pressure-cell simulation. Make time-history plots of gas saturation and CO₂ aqueous mass fraction and compare the results against those for the original pressure-cell simulation. Explain the observed differences.
2. (Moderate) Repeat the pressure-cell simulation, but altering the computational grid, either by altering the grid resolution (e.g., increasing the total number of nodes), or by altering the grid structure (e.g., keeping the total number of nodes constant and altering the grid spacing). Make time-history plots of gas saturation and CO₂ aqueous mass fraction and compare the results against those for the original pressure-cell simulation. Explain the observed differences.
3. (Difficult) Repeat the pressure-cell simulation using field-scale dimensions and grid resolution. Make time-history plots of gas saturation and CO₂ aqueous mass fraction and compare the results against those for the original pressure-cell simulation. Explain the observed differences.

Input Files

Scenario 1: Pressure-Cell Simulation Input File

~Simulation Title Card

1,
STOMP Example Problem CO2-7 Scenario 1,
M.D. White,
Pacific Northwest Laboratory,
10 June 2002,
11:09 AM PST,
2,
Pressure-cell simulation of supercritical CO2 injection
into pure water.

~Solution Control Card

Normal,
STOMP-CO2,
1,
0,day,6,hr,1.e-3,s,5,day,1.25,16,1.e-06,
1000,
Variable Aqueous Diffusion,
Variable Gas Diffusion,
0,

~Grid Card

Uniform Cartesian,
100,1,32,
0.17875,in,
0.5,in,
0.175781,in,

~Rock/Soil Zonation Card

1,
30/40 Accusand,1,100,1,1,1,32,

~Mechanical Properties Card

30/40 Accusand,2650,kg/m³,0.327,0.327,,,Millington and Quirk,

~Hydraulic Properties Card

30/40 Accusand,6.95,hc:cm/min,6.95,hc:cm/min,6.95,hc:cm/min,

~Saturation Function Card

30/40 Accusand,Brooks and Corey,19.06815,cm,8.476029,0.052,,

~Aqueous Relative Permeability Card

30/40 Accusand,Burdine,,

~Gas Relative Permeability Card

30/40 Accusand,Corey,,,

~Salt Transport Card

30/40 Accusand,0.0,m,0.0,m,

~Initial Conditions Card

Gas Pressure,Aqueous Pressure,
3,

Gas Pressure,138.0,Bar,,,,,,,,1,100,1,1,1,32,
Aqueous Pressure,138.0,Bar,,,,,,,,1,100,1,1,1,32,
Temperature,25.0,C,,,,,,,,1,100,1,1,1,32,

~Source Card

1,
Gas Volumetric Rate,Water-Vapor Mass Fraction,3,3,1,1,3,3,2,
0,hr,138.0,bar,8.5816,cm^3/hr,0.0,
4,hr,138.0,bar,8.5816,cm^3/hr,0.0,

~Boundary Conditions Card

1,
South,Aqu. Dirichlet,Gas Dirichlet,Aqu. Mass Frac.,
98,98,1,1,3,3,1,
0,s,138.0,bar,0.0,138.0,bar,1.0,0.0,,

~Output Options Card

3,
3,1,3,
10,1,32,
98,1,3,
1,1,hr,cm,6,6,6,
5,
Gas Saturation,,
Salt Saturation,,
Salt Aqueous Mass Fraction,,
CO2 Aqueous Mass Fraction,,
Gas Pressure,Bar,
1,
60@0.1,hr,
5,
Gas Saturation,,
Salt Saturation,,
Salt Aqueous Mass Fraction,,
CO2 Aqueous Mass Fraction,,
Gas Pressure,Bar,

Scenario 2: Hele-Shaw Simulation Input File

~Simulation Title Card

1,
STOMP Example Problem CO2-7 Scenario 2,
Sylvie Chevalier,
Masdar Institute,
11 May 2012,
11:09 AM PST,
2,
Simulation of viscous finger formation in a Hele-Shaw cell
from a heterogeneous initial distribution of dissolved CO2.

~Solution Control Card

Normal,
STOMP-CO2,
1,
0,day,2000,day,0.0001,day,5.,day,1.5,10,1.e-6,
1,hr,1,hr,30000,
variable aqueous Diffusion,
zero Gas Diffusion,
0,

~Grid Card

Cartesian,
100,1,150,
0,m,100@0.1,m,
0,m,1@1,m,
0,m,80@0.2,m,30@0.1,m,12@0.05,m,10@0.025,m,8@0.0125,m,10@0.005,m,

~Rock/Soil Zonation Card

1,
Geologic Media,1,100,1,1,1,150,

~Mechanical Properties Card

Geologic Media,,,0.2,0.2,4.5e-6,1/m,Millington and Quirk,

~Hydraulic Properties Card

Geologic Media,1.e-11,m²,,,1.e-11,m²,

~Saturation Function Card

Geologic Media,van Genuchten,0.2,1/cm,1.8,0.0,,,

~Aqueous Relative Permeability Card

Geologic Media,Mualem,,

~Gas Relative Permeability Card

Geologic media,Mualem,,

~Salt Transport Card

Geologic Media,0.0,m,0.0,m,

~Initial Conditions Card

Gas pressure, Aqueous Pressure,
5,
Aqueous Pressure,1.019522E+07,Pa,,,,,-9810.,1/m,1,100,1,1,1,150,
Gas Pressure,1.009522E+07,Pa,,,,,-9810.,1/m,1,100,1,1,1,150,
co2 relative saturation file,0.,,initialco2,

Temperature,45,C,,,,,1,100,1,1,1,150,
salt aqueous concentration,100.,kg / m³,,,,,,1,100,1,1,1,150,

~Surface flux Card

3,
CO2-Mass,kg / s,kg,Bottom,1,100,1,1,150,150,
Aqueous-Phase CO2 Mass,kg / s,kg,Bottom,1,100,1,1,150,150,
Gas-Phase CO2 Mass,kg / s,kg,Top,1,100,1,1,150,150,

~Boundary Conditions Card

1,
Top,initial condition,zero flux,zero flux,
1,100,1,1,150,150,1,
0,day,1.e+7,Pa,1.,1.e+7,Pa,0.,,,

~Output Control Card

4,
50,1,150,
50,1,1,
1,1,150,
100,1,150,
1,1,day,m,,,,
4,
Salt Aqueous Concentration,kg / m³,
CO2 Aqueous Concentration,kg / m³,
Aqueous saturation,,
gas saturation,,
13,
1.,day,
10,day,
50,day,
100,day,
200,day,
400,day,
600,day,
800,day,
1000,day,
1200,day,
1400,day,
1600,day,
1800,day,
8,
Salt Aqueous Concentration,kg / m³,
CO2 Aqueous Concentration,kg / m³,
aqueous density,,
Aqueous saturation,,
Aqueous Pressure,Pa,
gas saturation,,
gas pressure,Pa,
total CO2 mass,,

Solution to Selected Exercises

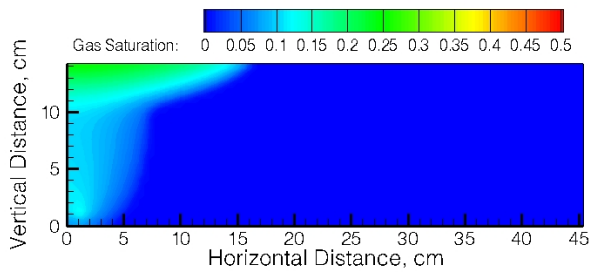
Exercise 1

The *invariant fluid density and viscosity* option in the *Solution Control Card* makes the aqueous and gas (i.e., CO₂ dominant phase) have constant density and viscosity during the simulation. When this option is invoked the aqueous and gas density and viscosity are specified in the *Solution Control Card*. To determine aqueous and gas density and viscosity, a single-node, zero-time-step simulation was executed at 138 bar and 45°C, with the aqueous and gas density and viscosity requested as output at the single reference node. The results from this simulation are shown in Table 3. The input file for this exercise is listed below.

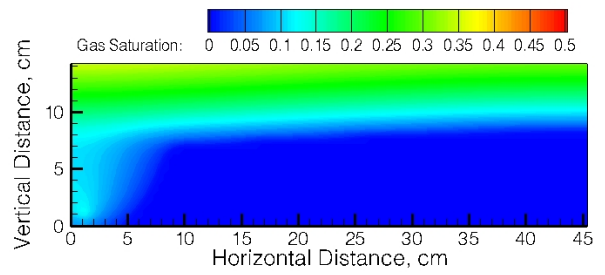
Table 3. Invariant aqueous and gas density and viscosity determined from a single-node, zero-time-step simulation at 138 bar and 45°C

Phase	Properties
Aqueous	$\rho_l = 1003.28 \text{ kg / m}^3 ; \mu_l = 8.9769 \times 10^{-4} \text{ Pa s}$
Gas	$\rho_g = 863.142 \text{ kg / m}^3 ; \mu_g = 8.2673 \times 10^{-5} \text{ Pa s}$

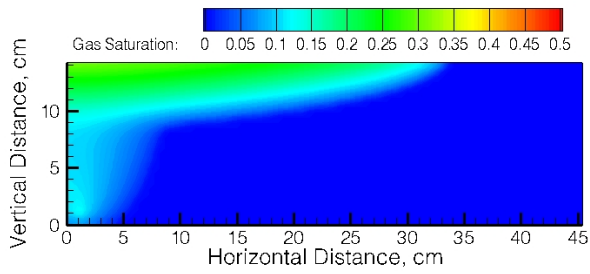
With invariant fluid properties, the aqueous density does not change with CO₂ dissolution. This does not greatly impact the gas saturation profiles, as shown in Figure 4, with the exception of the elevation of the aqueous-gas transition point at the final time step, which is lower than for the base simulation with variable density. This indicates more CO₂ remains in the gas phase. The dissolved CO₂ profiles, shown in Figure 5, are starkly different from those in Figure 2, as no viscous fingers form. This is due to the lack of a density instability, as the aqueous density is independent of dissolved CO₂ concentration. The lack of a density instability results in less mixing and a smaller fraction of the total CO₂ being dissolved in the aqueous phase.



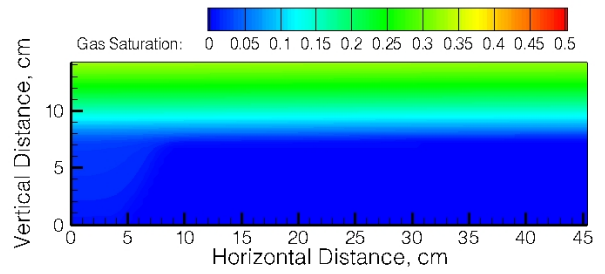
4a



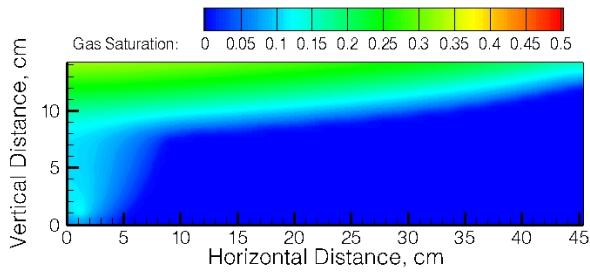
4d



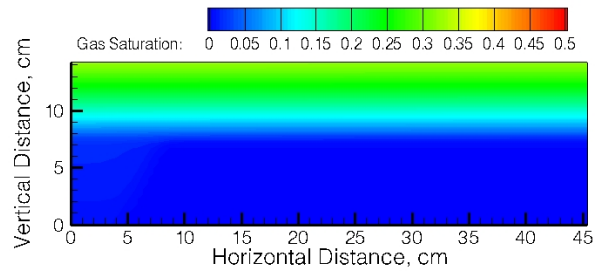
4b



4e



4c



4f

Figure 4. Exercise 1: Gas Saturation Profiles at 1, 2, 3, 4, 5, and 6 Hours in 4a, 4b, 4c, 4d, 4e, and 4f, Respectively

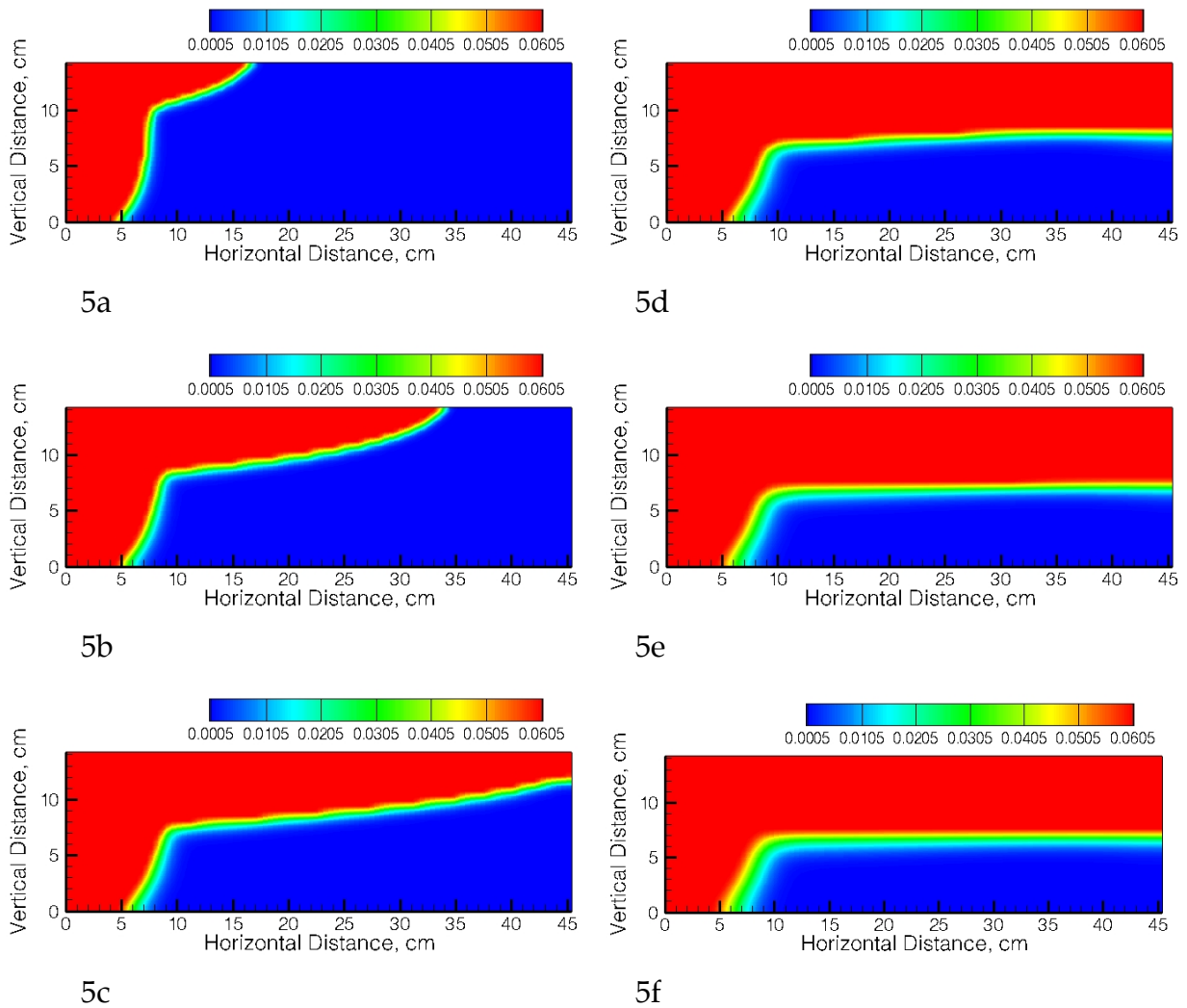


Figure 5. Exercise 1: CO₂ Aqueous Mass Fraction Profiles at 1, 2, 3, 4, 5, and 6 Hours in 5a, 5b, 5c, 5d, 5e, and 5f, Respectively

Input Files

Scenario 1: Exercise 1 Input File

~Simulation Title Card

1,
STOMP Example Problem CO2-7: Exercise 1,
M.D. White,
Pacific Northwest Laboratory,
10 June 2002,
11:09 AM PST,
2,
Pressure-cell simulation of supercritical CO2 injection
into pure water.

~Solution Control Card

Normal,
STOMP-CO2 w/ Invariant Fluid Density and Viscosity,
1,
0,day,6,hr,1.e-3,s,5,day,1.25,16,1.e-06,
1000,
Variable Aqueous Diffusion,
Variable Gas Diffusion,
1003.28,kg/m³,8.9769e-4,Pa s,863.142,kg/m³,8.2673e-5,Pa s,
0,

~Grid Card

Uniform Cartesian,
100,1,32,
0.17875,in,
0.5,in,
0.175781,in,

~Rock/Soil Zonation Card

1,
30/40 Accusand,1,100,1,1,1,32,

~Mechanical Properties Card

30/40 Accusand,2650,kg/m³,0.327,0.327,,,Millington and Quirk,

~Hydraulic Properties Card

30/40 Accusand,6.95,hc:cm/min,6.95,hc:cm/min,6.95,hc:cm/min,

~Saturation Function Card

30/40 Accusand,Brooks and Corey,19.06815,cm,8.476029,0.052,,

~Aqueous Relative Permeability Card

30/40 Accusand,Burdine,,

~Gas Relative Permeability Card

30/40 Accusand,Corey,,,

~Salt Transport Card

30/40 Accusand,0.0,m,0.0,m,

~Initial Conditions Card

Gas Pressure,Aqueous Pressure,
3,

Gas Pressure,138.0,Bar,,,,,,,,1,100,1,1,1,32,
Aqueous Pressure,138.0,Bar,,,,,,,,1,100,1,1,1,32,
Temperature,25.0,C,,,,,,,,1,100,1,1,1,32,

~Source Card

1,
Gas Volumetric Rate,Water-Vapor Mass Fraction,3,3,1,1,3,3,2,
0,hr,138.0,bar,8.5816,cm^3/hr,0.0,
4,hr,138.0,bar,8.5816,cm^3/hr,0.0,

~Boundary Conditions Card

1,
South,Aqu. Dirichlet,Gas Dirichlet,Aqu. Mass Frac.,
98,98,1,1,3,3,1,
0,s,138.0,bar,0.0,138.0,bar,1.0,0.0,,

~Output Options Card

3,
3,1,3,
10,1,32,
98,1,3,
1,1,hr,cm,6,6,6,
9,
Aqueous Density,,
Aqueous Viscosity,,
Gas Density,,
Gas Viscosity,,
Gas Saturation,,
Salt Saturation,,
Salt Aqueous Mass Fraction,,
CO2 Aqueous Mass Fraction,,
Gas Pressure,Bar,
1,
60@0.1,hr,
9,
Aqueous Density,,
Aqueous Viscosity,,
Gas Density,,
Gas Viscosity,,
Gas Saturation,,
Salt Saturation,,
Salt Aqueous Mass Fraction,,
CO2 Aqueous Mass Fraction,,
Gas Pressure,Bar,